Biophysical Journal, Volume *120*

Supplemental information

Biophysical properties of corneal cells reflect high myopia progression

Ying Xin, Byung Soo Kang, Yong-Ping Zheng, Sze Wan Shan, Chea-su Kee, and Youhua Tan

Supplementary Figures

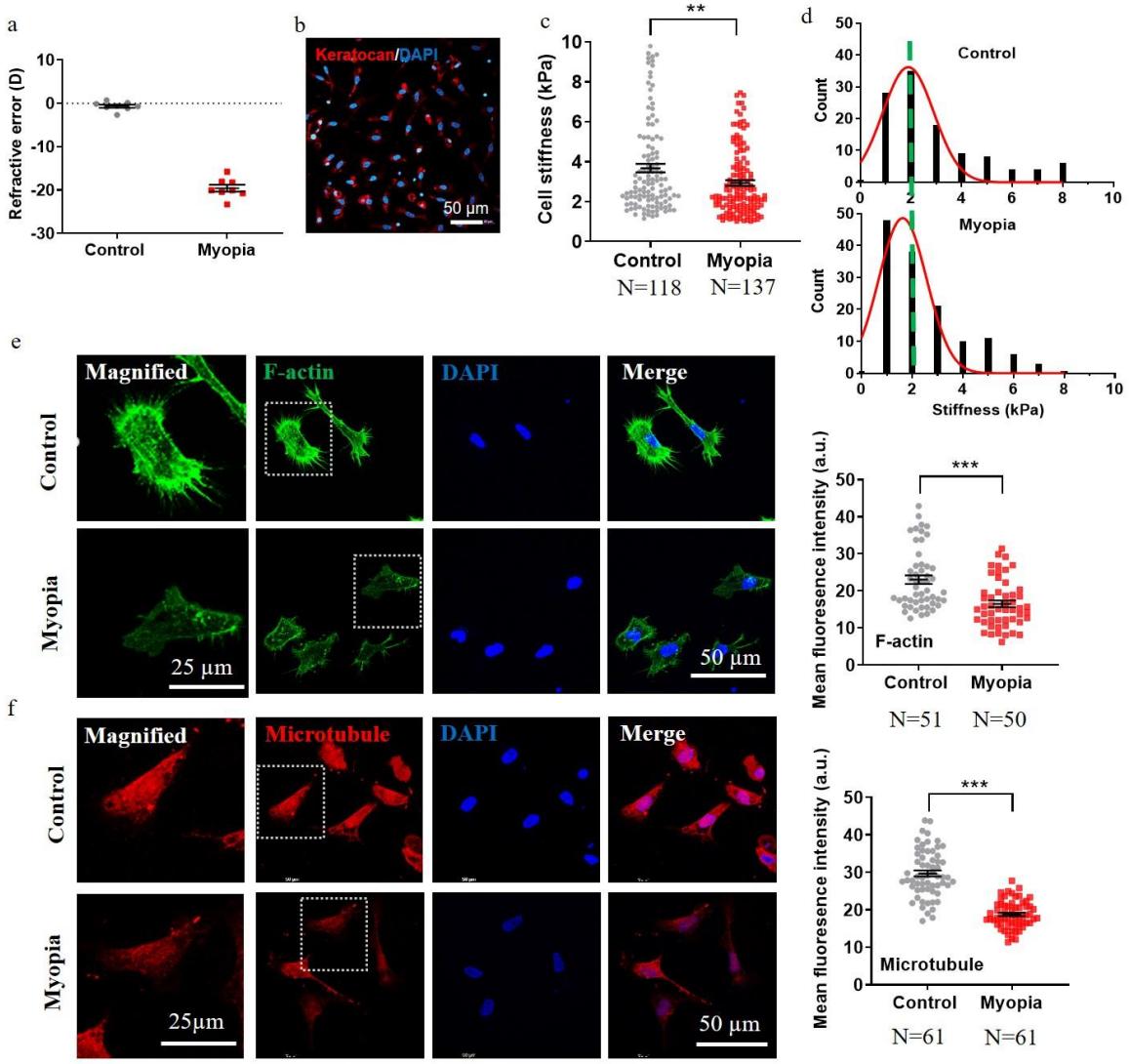

Figure S1 Myopic corneal cells exhibit reduced F-actin/microtubule and cellular stiffness in the LIM model. (a) Refractive state after the LIM treatment. Representative of at least three independent experiments. (b) Immunofluorescence staining of Keratocan in cornea-derived cells. (c) Myopic corneal cells are softer than control cells. Representative of three independent experiments. (d) The histogram of cellular stiffness in (c). (e, f) Myopic corneal cells exhibit reduced F-actin and microtubule. Representative of three independent experiments. Scale bar: 50 μm in the non-magnified images and 25 μm in the magnified images. **, $p<0.01$; ***, $p<0.001$.

a

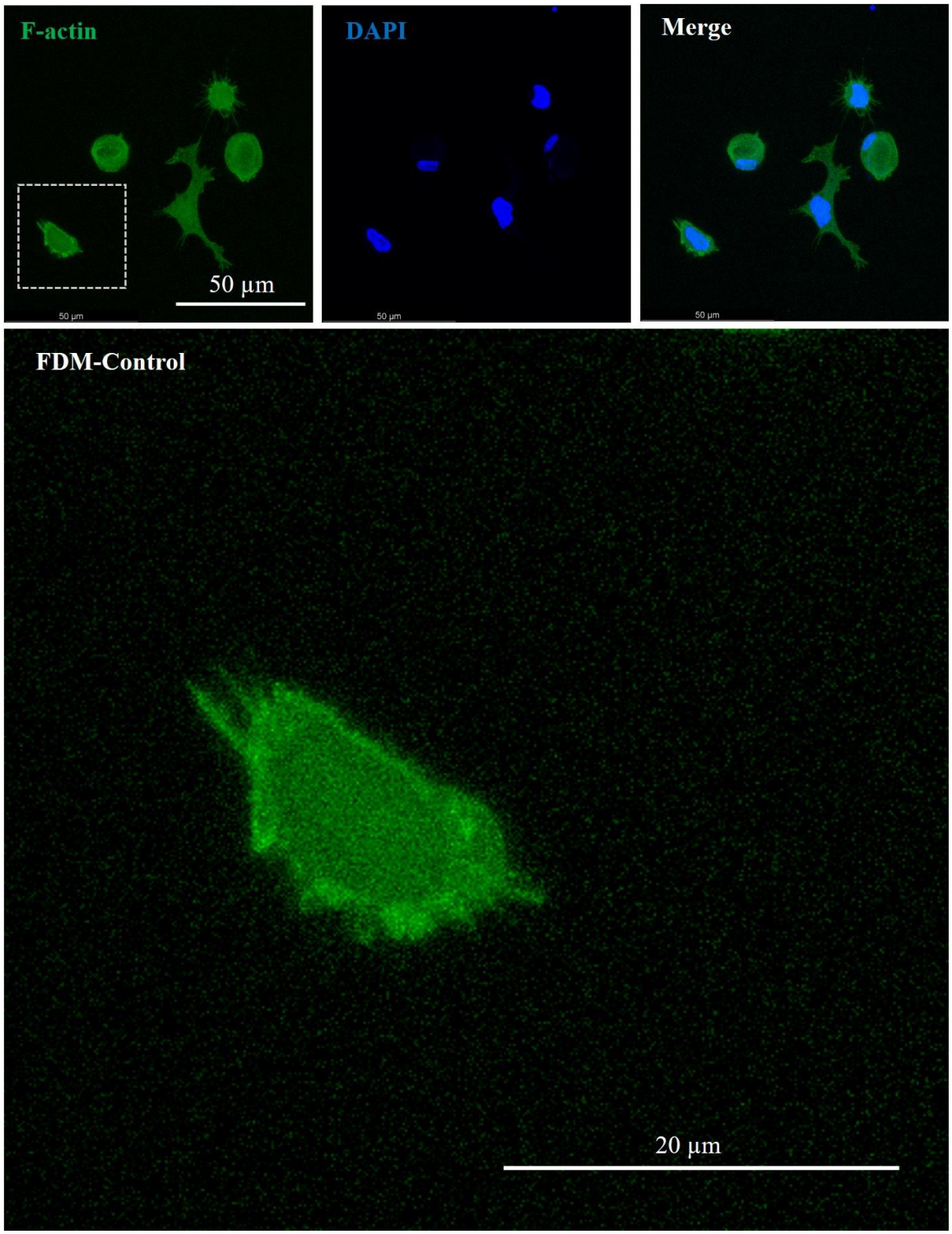

b

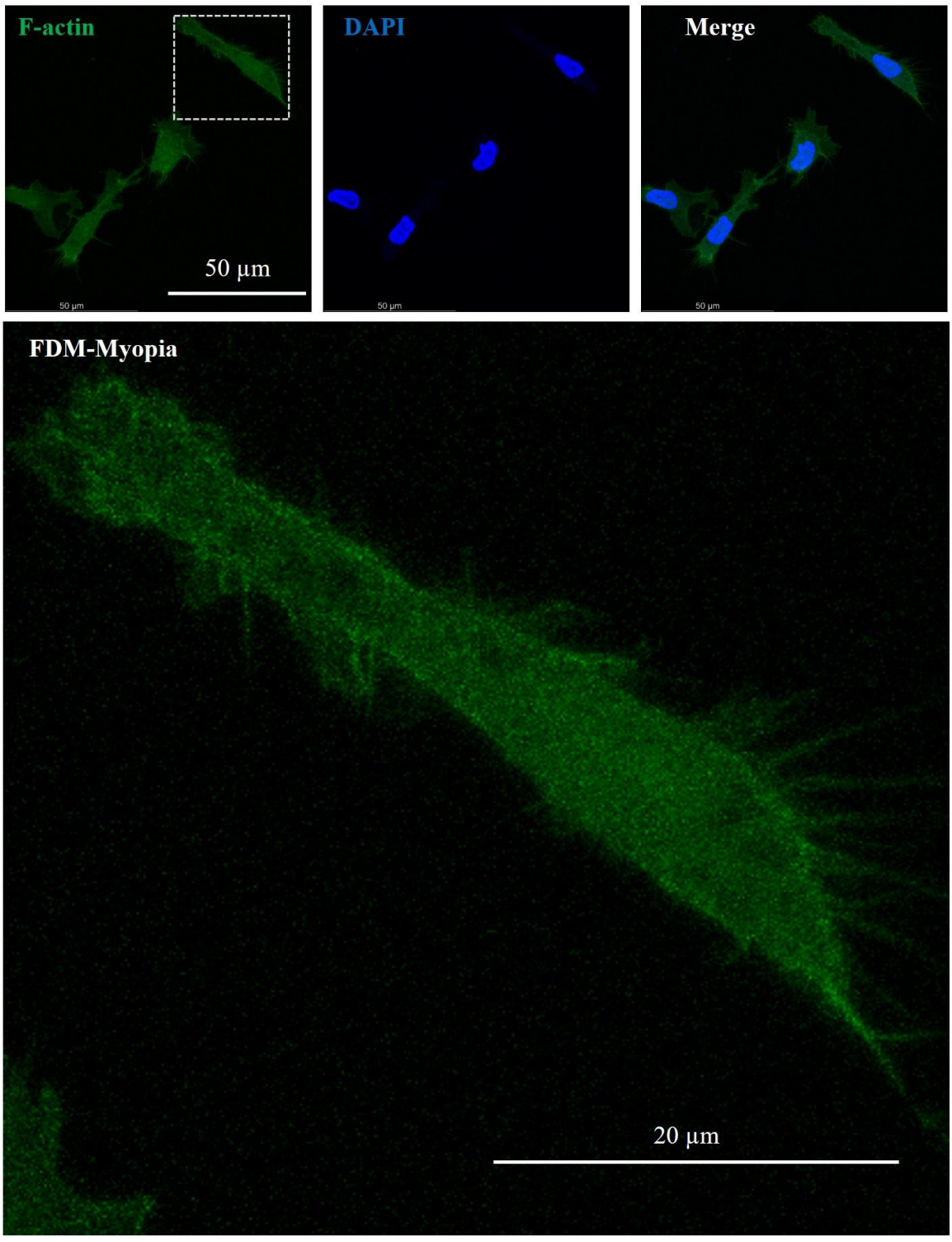

c

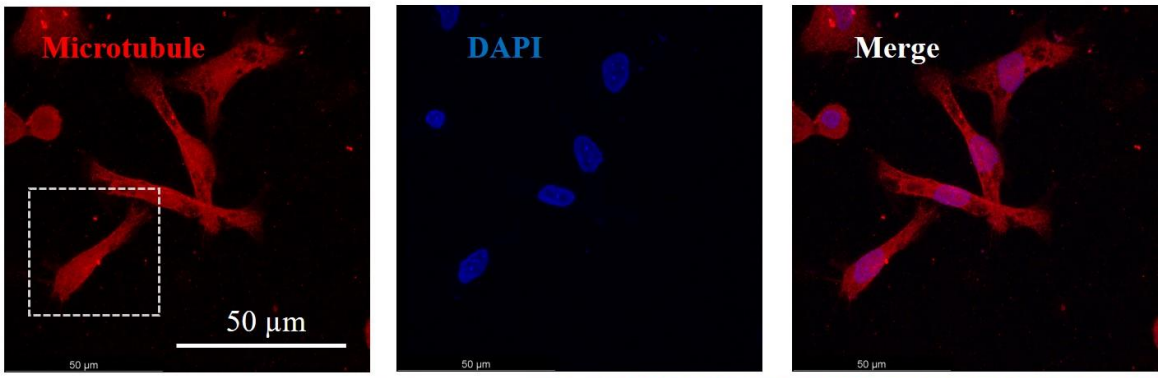

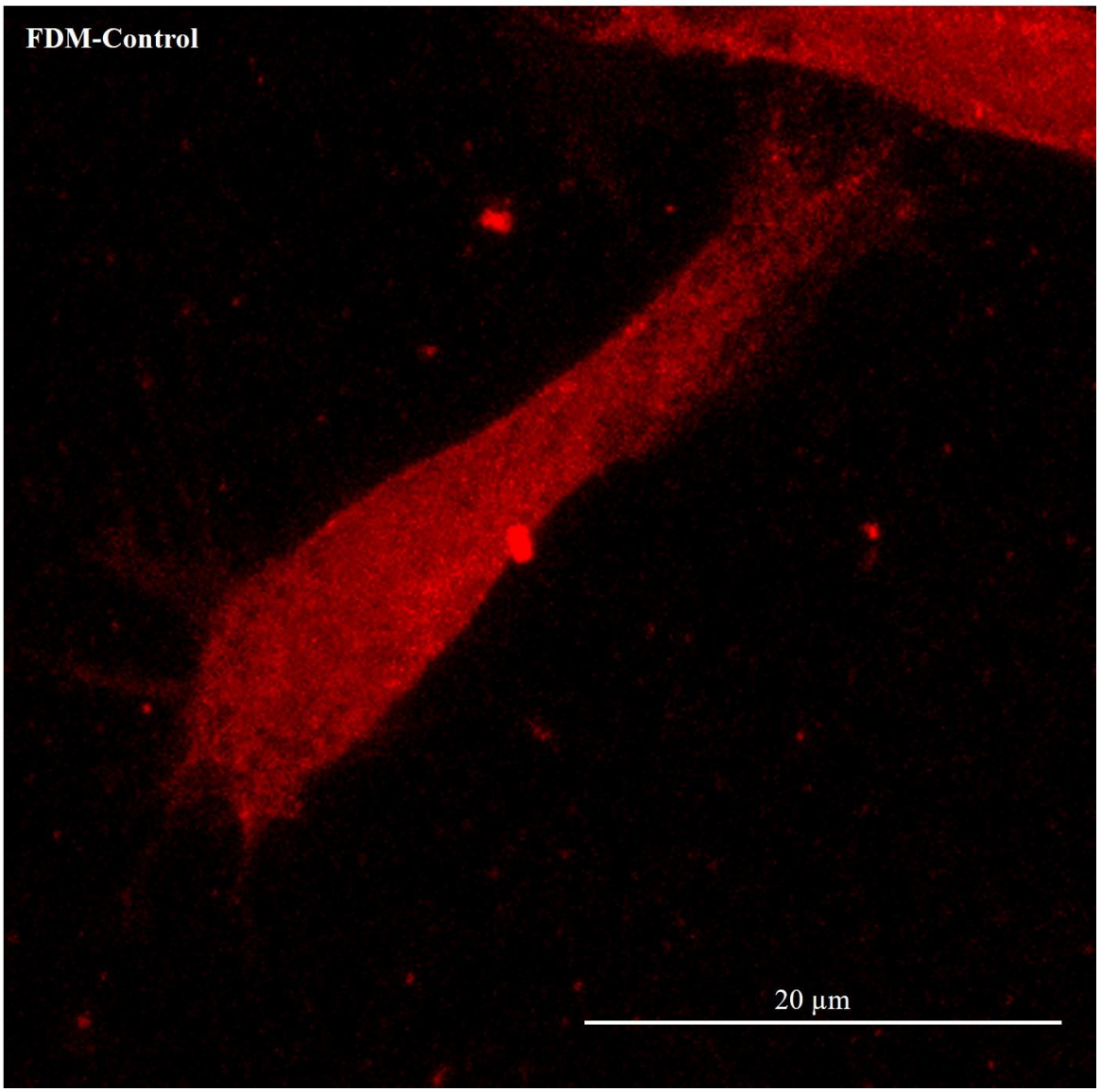

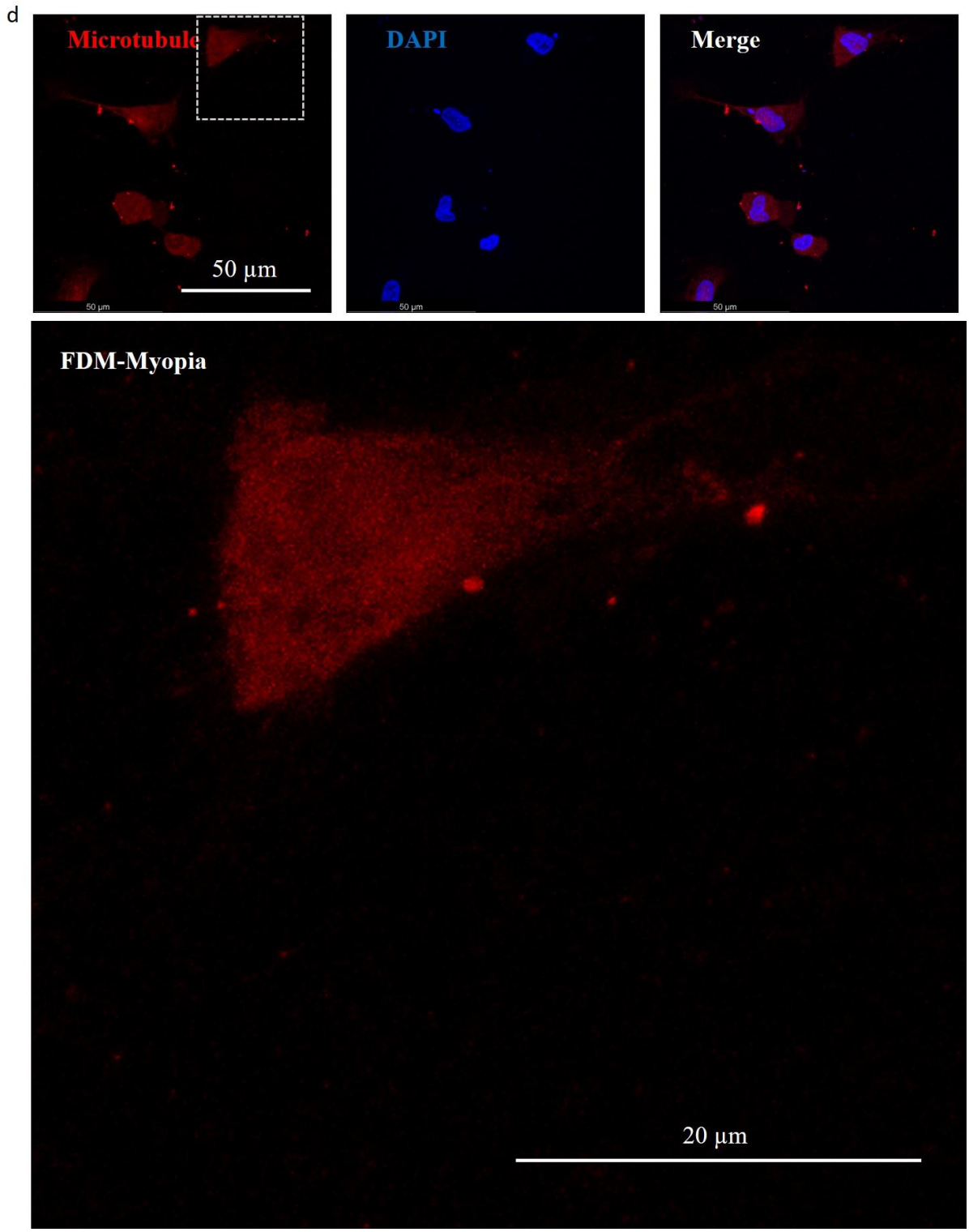

Figure S2 Myopic corneal cells exhibit reduced F-actin and microtubule in the FDM model.

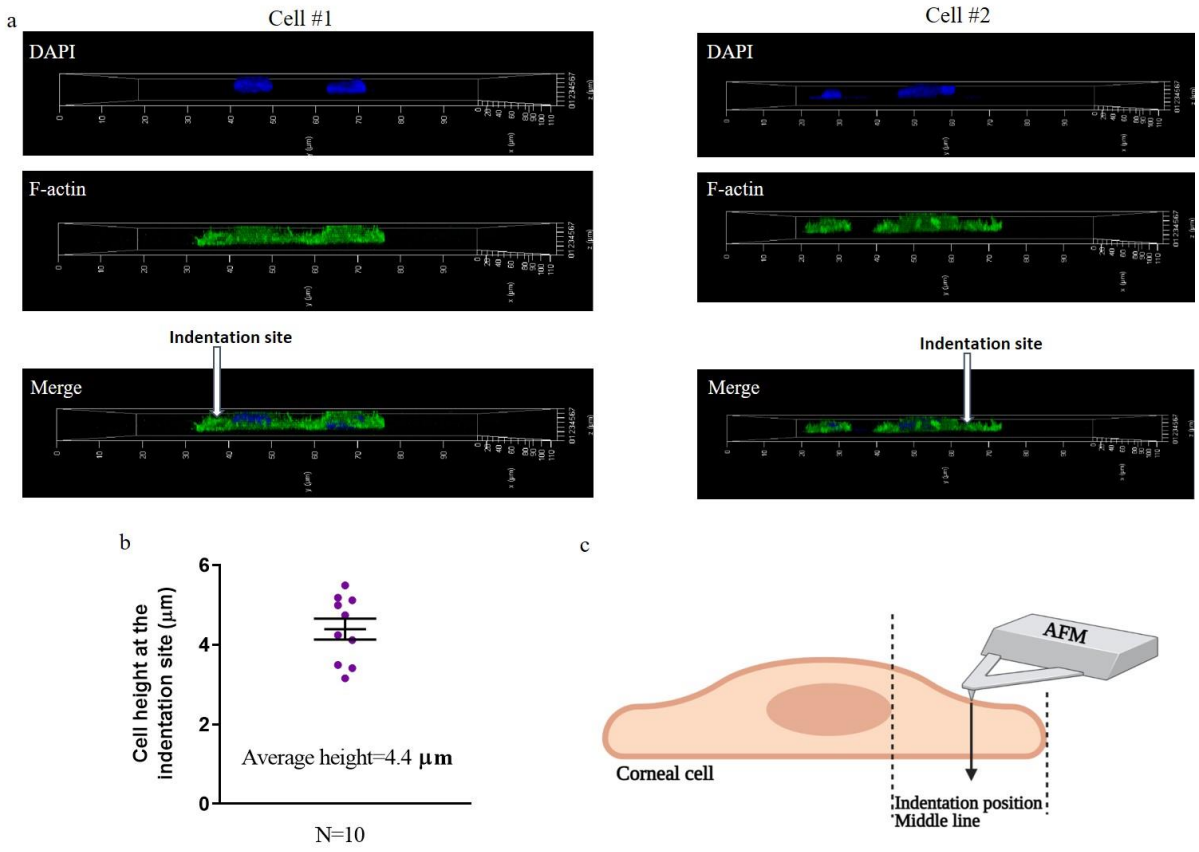

Figure S3 The stiffness measurement of corneal cells by AFM. (a) The actin and nucleus were stained with phalloidin and DAPI in corneal cells and then imaged by confocal microscope. The 3D structure of the cells was re-constructed by the software Leica LAS X. (b) The cellular area that was near the middle between the nucleus and cell periphery was chosen for stiffness measurement as indicated in the bottom panel, where cell thickness was ~4.4 μm. (c) The schematic of cell indentation by AFM.

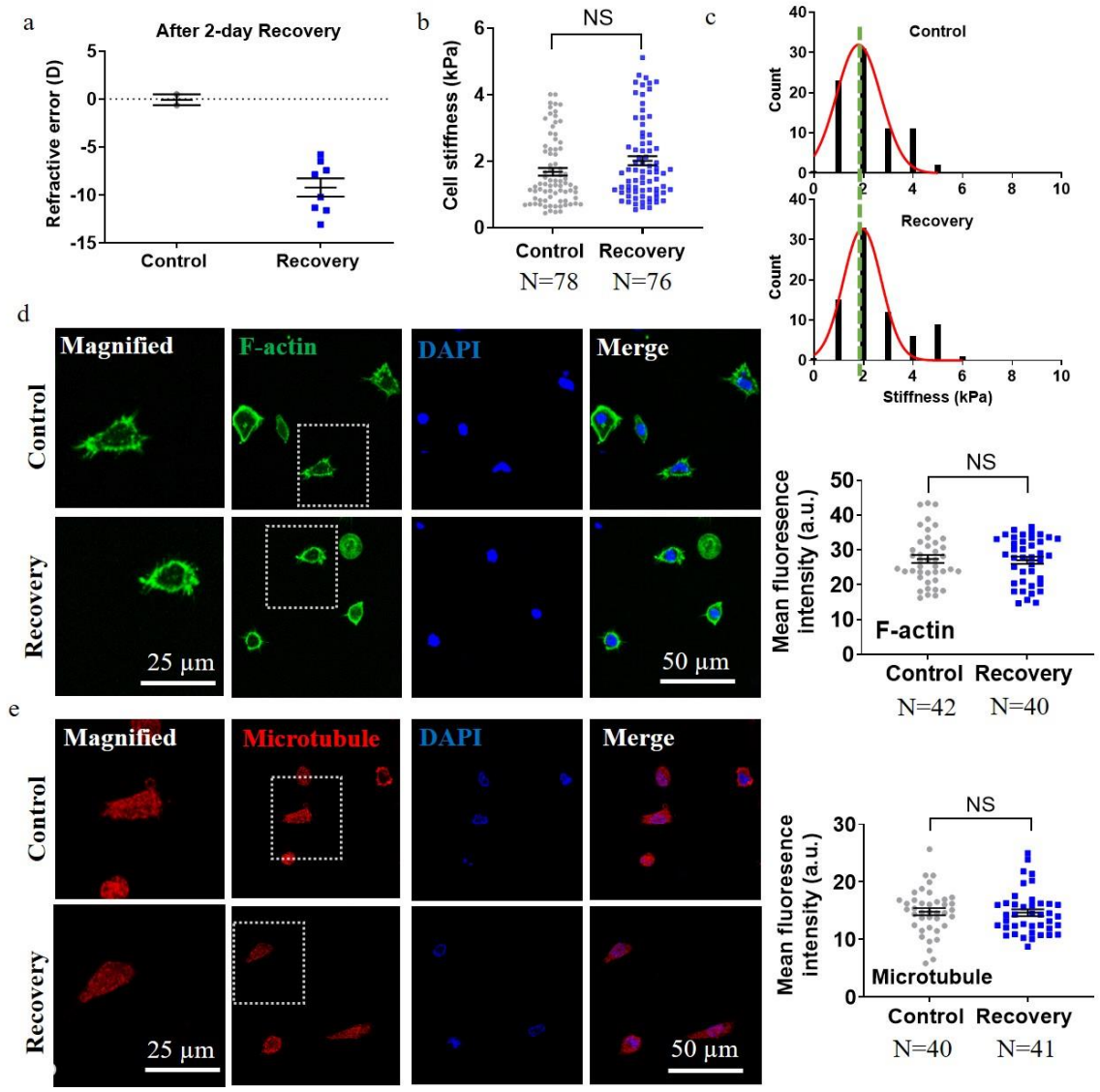

Figure S4 F-actin/microtubule and cellular stiffness of myopic corneal cells are restored to the levels of control cells after recovery in the LIM model. (a) The refractive state after recovery. Representative of at least three independent experiments. (b) Myopic corneal cells exhibit similar stiffness to control cells after recovery. NS: no significance. n=3. (c) The histogram of cell stiffness in (b). (d, e) Recovered corneal cells show similar F-actin/microtubule compared to control cells. The representative images were shown and the fluorescence intensity was quantified in the right panel. Representative of three independent experiments.

a

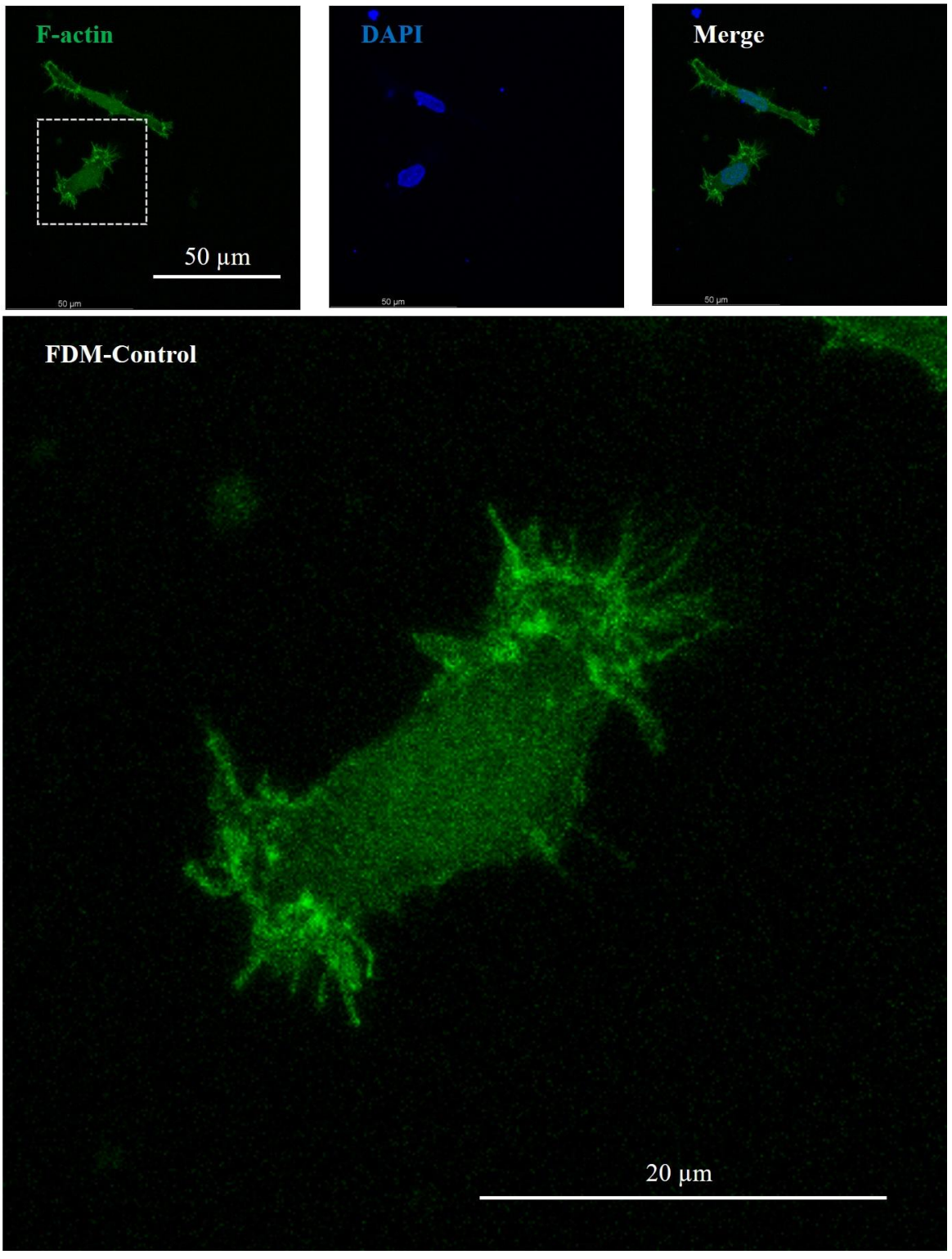

b

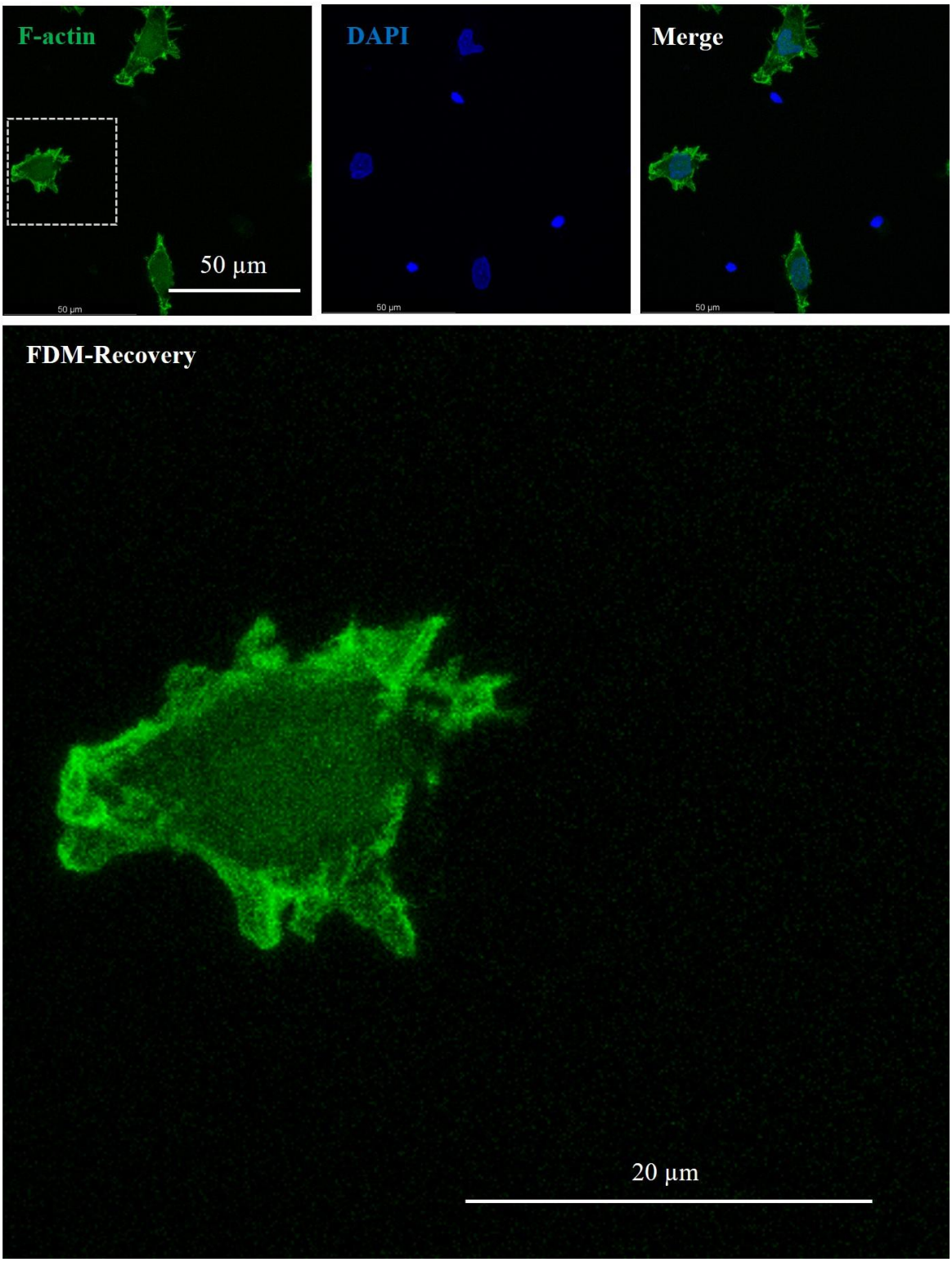

c

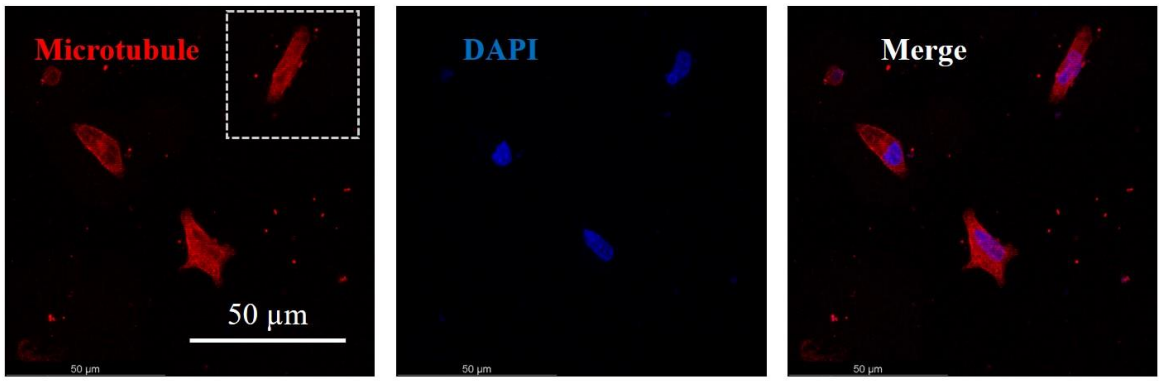

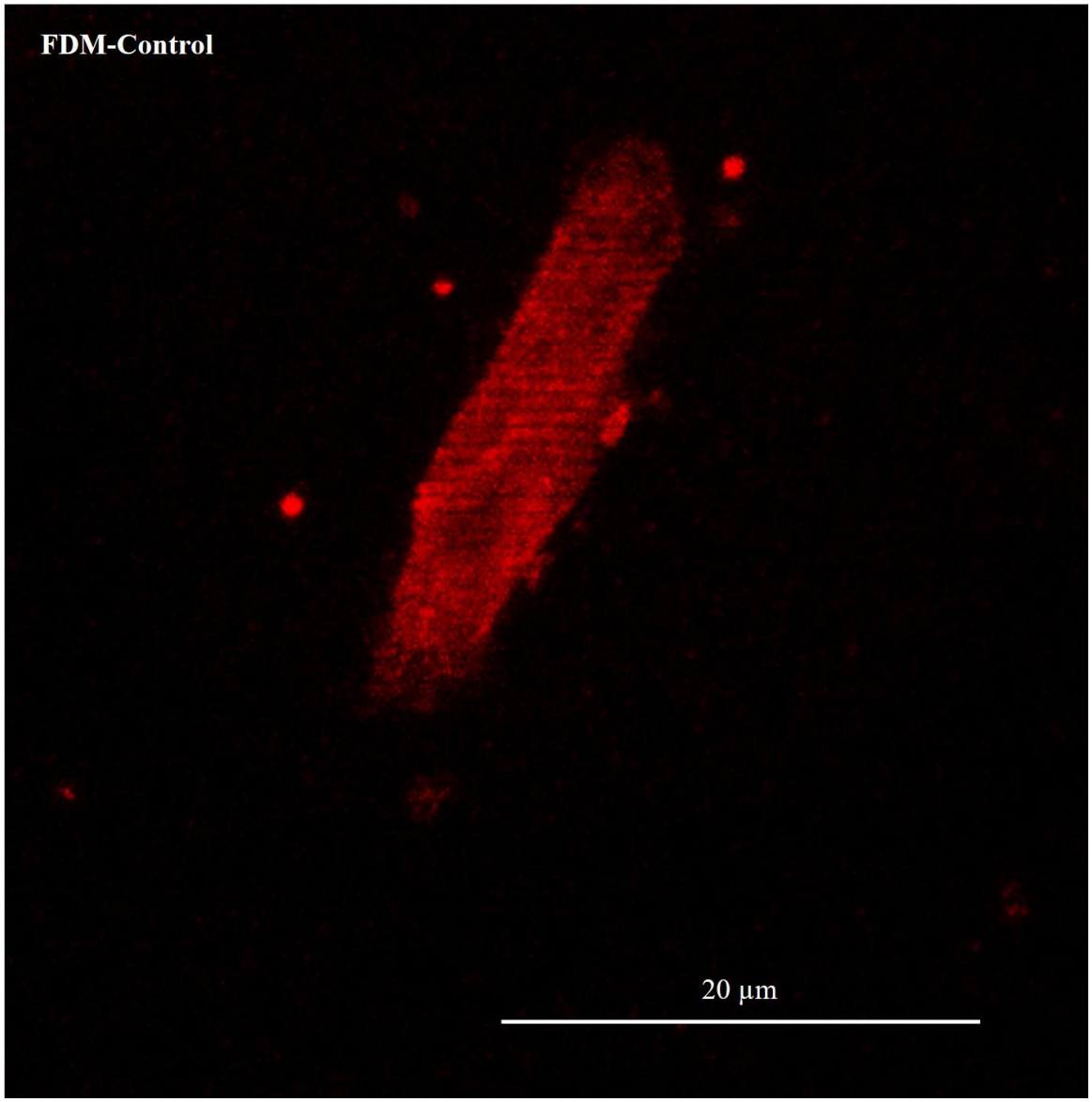

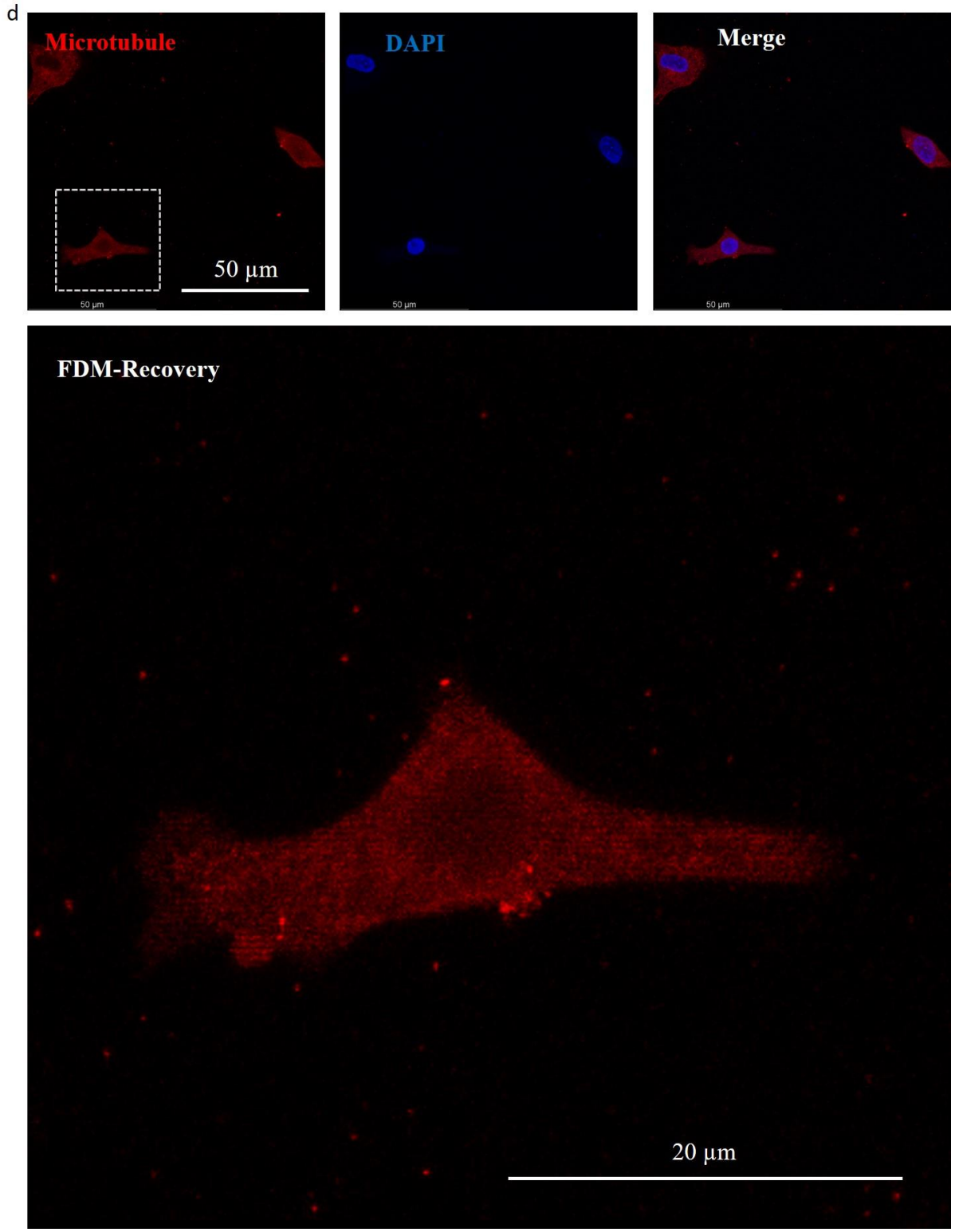

Figure S5 F-actin and microtubule of myopic corneal cells are partially restored to the levels of control cells after recovery in the FDM model.

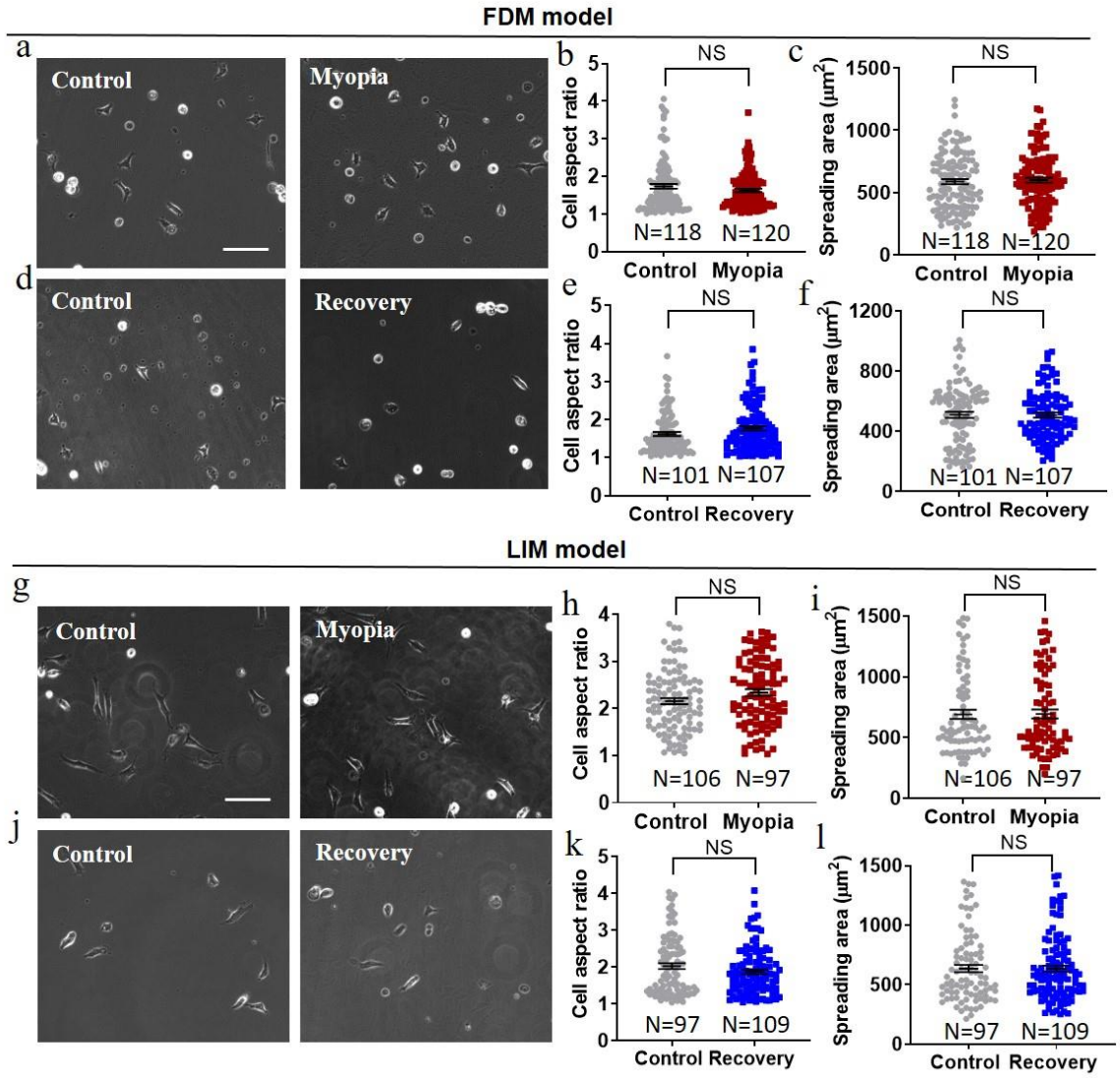

Figure S6 There is no obvious difference in the morphology of normal, myopic, and recovered corneal cells. (a-c, g-i) Myopic corneal cells and control cells exhibit similar morphology. Myopic cells and control cells from both FDM (a-c) and LIM (g-i) were plated on glass for 24 h and cell images were captured for the quantification of cell aspect ratio (b, h) and area (c, i). (d-f, j-l) Myopic cells after recovery exhibit similar morphology to control cells. Myopic cells after recovery and control cells from both FDM (d-f) and LIM (j-l) were plated on glass for 24 h and cell images were captured for the quantification of cell aspect ratio (e, k) and area (f, l). Representative of three independent experiments. NS: no significance. Scale bar: 100 μm.

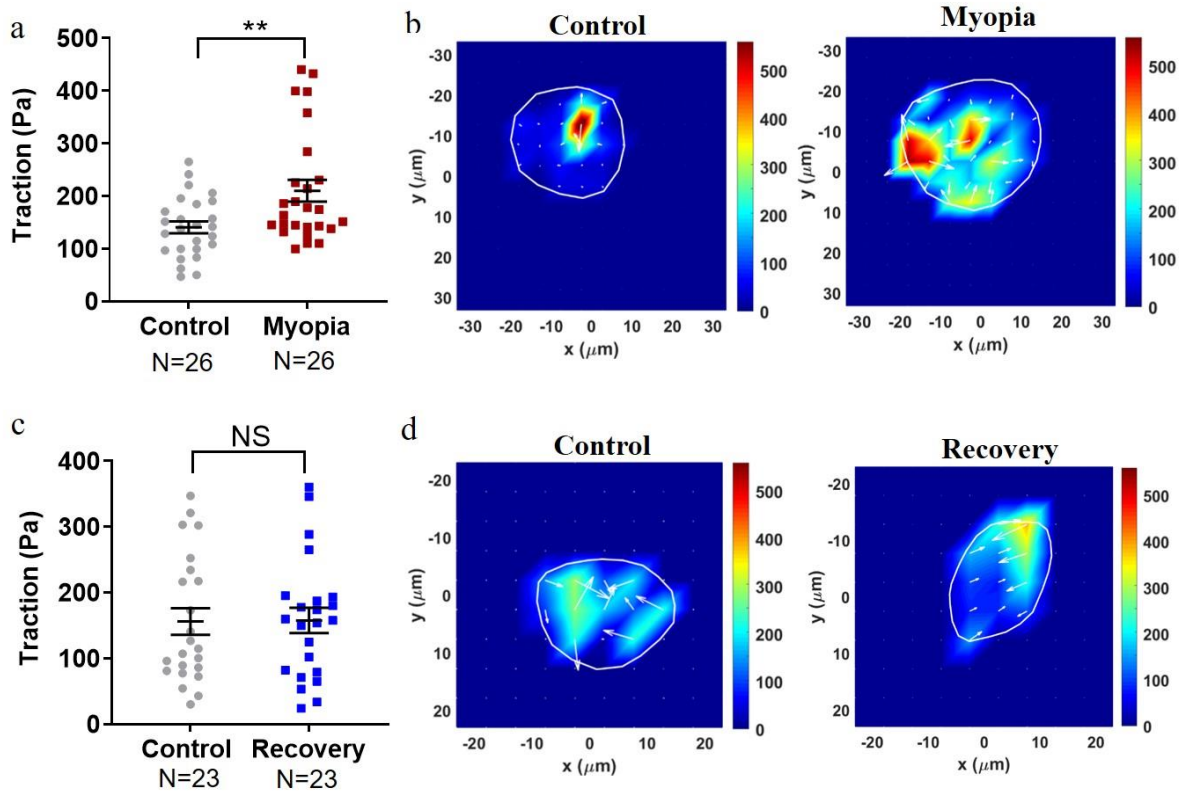

Figure S7 Traction force is elevated in myopic cells and restored to the level of control cells after recovery in the LIM model. (a) Myopic cells generate elevated traction force compared to control corneal cells. n=3 independent experiments. **, $p<0.01$. (b) Representative images of traction force in control and myopic cells. (c) Myopic cells generate similar traction force to control cells after recovery. n=3 independent experiments. NS: no significance. (d) Representative images of traction force in control and recovered cells.

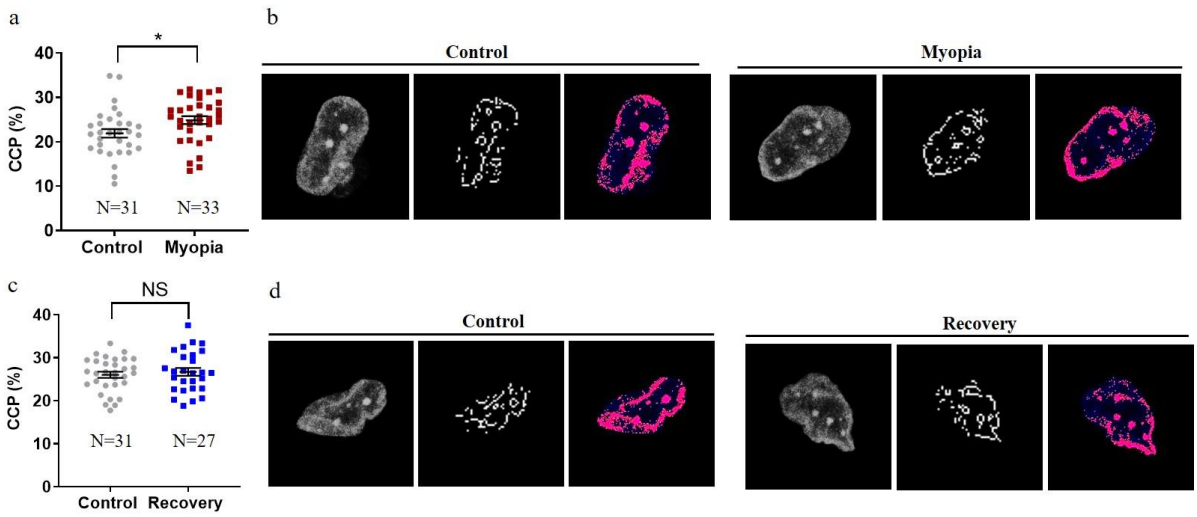

Figure S8 Myopic corneal cells increase chromatin condensation in the nucleus that is restored to the level of healthy cells after recovery in the LIM model. (a) Myopic corneal cells exhibit higher level of chromatin condensation than control cells. The chromatin condensation parameter (CCP) of both myopic and control corneal cells was measured to represent the level of chromatin condensation. n=32 cells. Representative of three independent experiments. *, $p<0.05$. (b) Representative images of chromatin condensation in myopic and control cells. The nuclei of both myopic corneal cells and control cells were stained with DAPI (left panel). The visible edges within the nucleus were identified by CCP image processing (middle panel) and the condensed nuclear area was filled with pseudo color (right panel). (c) Recovered cells exhibit similar level of chromatin condensation to control cells. n=32 cells. Representative of three independent experiments. NS: no significance. (d) Representative images of chromatin condensation in recovered and control cells.